

Parallel Polyhedral Projection Method for the Convex Feasibility Problem

Pablo Barros

School of Applied Mathematics, FGV
Praia de Botafogo, Rio de Janeiro, Brazil
pabloacbarros@gmail.com

Vincent Guigues

School of Applied Mathematics, FGV
Praia de Botafogo, Rio de Janeiro, Brazil
vincent.guigues@fgv.br

Roger Behling

Department of Mathematics, UFSC
Blumenau, SC, Brazil
rogerbehling@gmail.com

Abstract

In this paper, we introduce and study the Parallel Polyhedral Projection Method (3PM) and the Approximate Parallel Polyhedral Projection Method (A3PM) for finding a point in the intersection of finitely many closed convex sets. Each iteration has two phases: parallel projections onto the target sets (exact in 3PM, approximate in A3PM), followed by an exact or approximate projection onto a polyhedron defined by supporting half-spaces. These strategies appear novel, as existing methods largely focus on parallel schemes like Cimmino’s method. Numerical experiments demonstrate that A3PM often outperforms both classical and recent projection-based methods when the number of sets is greater than two. Theoretically, we establish global convergence for both 3PM and A3PM without regularity assumptions. Under a Slater condition or error bound, we prove linear convergence, even with inexact projections. Additionally, we show that 3PM achieves superlinear convergence under suitable geometric assumptions.

Key words. Convex feasibility problem, Projection and reflection operators, Optimization algorithms

AMS subject classifications. ???

1 Introduction

The Convex Feasibility Problem involves finding a point within the intersection $U \neq \emptyset$ of a finite collection of closed convex sets $\{U_i\}_{i=1}^m$, that is

$$\text{find } u^* \in U := \bigcap_{i=1}^m U_i. \quad (1)$$

Finding a point in the intersection of finitely many closed convex sets is a fundamental task that serves as a modeling paradigm in numerous computational settings. Projection algorithms have long been prominent for these problems, dating back to the seminal method of simultaneous (parallel) projections by Cimmino (1938) [18]. Cimmino’s algorithm introduced the idea of averaging projections onto all constraint sets at each iteration, an approach that proved influential in early applications such as computerized tomography; see Combettes [19]. Another cornerstone is the Douglas–Rachford (DR) method, an iterative reflection scheme that has become a popular solver for convex feasibility and related optimization problems (Bauschke and Combettes [7]; Borwein and Sims [17]; Aragón Artacho et al. [3]; Bauschke et al. [10]; Phan [29]; Bauschke and Moursi [11]).

In recent years, novel enhancements of these classical techniques have emerged (Aragón Artacho and Campoy [2]; Lu and Zhang [27]; Torun et al. [34]; Duff et al. [21]). Notably, the circumcentered-reflection method (CRM) was proposed as a geometrically inspired acceleration of projection algorithms, computing the circumcenter of several reflected points to jump closer to the solution set (Behling et al. [15]; Behling et al. [14]; Bauschke et al. [9]). The CRM can dramatically outperform the standard DR method in certain settings (e.g., affine subspaces), enjoying linear convergence under appropriate conditions (Behling et al. [13]; Behling et al. [12]). Beyond CRM, many recent works have developed randomized and block-iterative projection schemes that leverage parallel computing architectures and offer improved convergence guarantees (Necoara et al. [28]; Han et al. [23]; Kolobov et al. [24]).

The continued interest in projection methods (Scolnik et al. [32]; Shen et al. [33]; Li and Pong [26]) stems from their wide-ranging applications, including gene regulatory network inference (Wang et al. [35]), large-scale signal processing (Combettes and Pesquet [20]), and even combinatorial optimization problems reformulated as feasibility problems (Aragón Artacho et al. [1]). Within this rich landscape of algorithms, the *Parallel Polyhedral Projection Method* (3PM) advances the state of the art by adopting a fully simultaneous projection scheme in the spirit of Ciminio’s method, while incorporating modern geometric strategies inspired by the Douglas–Rachford and Circumcentered Reflection methods to enhance robustness and accelerate convergence.

In this work, we introduce the 3PM algorithm, along with its inexact variant A3PM. Each iteration of both methods is structured into two phases:

1. Compute the (exact or approximate) projections $P_{U_1}(x), P_{U_2}(x), \dots, P_{U_m}(x)$ of the current iterate x onto each of the sets U_i ;
2. Define the next iterate as the (exact or approximate) projection of x onto the polyhedron $\Omega := \bigcap_{i=1}^m S_i$, where each supporting half-space is given by

$$S_i := \{z \in \mathbb{R}^n \mid \langle x - P_{U_i}(x), z - P_{U_i}(x) \rangle \leq 0\}.$$

Although conceptually simple, this two-phase strategy is new, to the best of our knowledge.

The main contributions of this work are as follows:

Parallel Polyhedral Projection Method. We propose the *Parallel Polyhedral Projection Method* (3PM), a new approach for solving the convex feasibility problem (1). At each iteration, 3PM performs parallel projections onto the target sets and then computes a single projection onto a polyhedron defined by affine half-spaces supporting the sets at the projected points. We prove that 3PM converges globally without requiring any regularity assumptions. Moreover, if the intersection U satisfies an error bound condition, which is guaranteed when $\text{int}(U) \neq \emptyset$, then the method achieves a linear convergence rate. Under additional geometric conditions, we show that 3PM exhibits superlinear convergence.

Inexact Variant A3PM. We introduce A3PM, an inexact version of 3PM in which both the parallel and polyhedral projections may be computed approximately. This generalization retains the convergence guarantees of 3PM: global convergence is preserved even without regularity, and linear convergence is ensured under standard error bound conditions. This makes A3PM suitable for applications where exact projections are impractical or costly.

Numerical experiments. We present numerical experiments for the problem of finding a point in an intersection of ellipsoids. The results highlight the competitive performance of A3PM in comparison to classical and modern projection methods such as CRM, Cyclic projections, Ciminio’s method, and Successive Centralized CRM (SCCRM) from Behling et al. [30], particularly in settings with more than two sets.

This paper is organized as follows. Section 2 is devoted entirely to the Parallel Polyhedral Projection Method (3PM): we describe the method, analyze its convergence properties, and relate it to classical projection methods. Section 3 introduces A3PM, an inexact variant of 3PM that allows for approximate projections in both algorithmic phases. We establish convergence guarantees for A3PM under mild assumptions, and

demonstrate that its theoretical properties mirror those of the exact version. Finally, in Section 4, we present numerical experiments that benchmark the performance of 3PM and A3PM against a selection of classical and recent projection algorithms.

1.1 Basic definitions and notation

We denote by \mathbb{R}^n the standard n -dimensional Euclidean space, equipped with the inner product $\langle \cdot, \cdot \rangle$ and associated norm $\|\cdot\|$. Given a nonempty, closed convex set $C \subset \mathbb{R}^n$, the projection of a point $x \in \mathbb{R}^n$ onto C is denoted by $P_C(x)$, and is defined as the unique point in C closest to x , that is,

$$P_C(x) := \operatorname{argmin}_{y \in C} \|x - y\|.$$

The distance from x to C is denoted by

$$\operatorname{dist}(x, C) := \inf_{y \in C} \|x - y\|.$$

Throughout the paper, we assume that the sets $U_1, \dots, U_m \subset \mathbb{R}^n$ are closed, convex, and nonempty. Their intersection is denoted by $U := \bigcap_{i=1}^m U_i$, which we assume is nonempty.

2 Parallel Polyhedral Projection Method for convex feasibility problems (3PM)

2.1 3PM method

In this section, we describe a new cutting plane method for the convex feasibility problem (1). We start from an arbitrary point $x_1 = x$ and for iteration $k \geq 1$, given x_k , we compute the projection $P_{U_i}(x_k)$ of x_k onto U_i for every i . Then let

$$S_{ik} = \left\{ z : \langle x_k - P_{U_i}(x_k), z - P_{U_i}(x_k) \rangle \leq 0 \right\} \quad (2)$$

be a half space that contains U_i , built from a separating hyperplane for U_i , and let

$$\Omega_k = \bigcap_{i=1}^m S_{ik}. \quad (3)$$

We compute the next iterate x_{k+1} as $x_{k+1} = P_{\Omega_k}(x_k)$ for Ω_k given by (3). The steps of 3PM are summarized in Algorithm 1 below.

This two-step process decouples the iteration into a first phase of identifying plausible corrections via individual projections, followed by a second phase in which the algorithm consolidates this information by projecting onto the polyhedron Ω_k . This region can be seen as a local outer approximation of the feasible set, built from first-order information about each U_i . The final projection thus performs a coordinated movement informed by all constraints, offering a sharper descent than methods based on single-set updates.

Figure 1 illustrates the computation of an iteration of 3PM for 3 sets U_1 , U_2 , and U_3 in \mathbb{R}^2 . In this figure we represent:

- convex sets U_1 , U_2 , and U_3 and their intersection U ;
- an arbitrary initial point x ;
- the projections $P_{U_1}(x)$, $P_{U_2}(x)$, and $P_{U_3}(x)$ of x onto respectively U_1 , U_2 , and U_3 ;
- half-spaces S_1 , S_2 , and S_3 which play the role of half-spaces S_{ik} in 3PM; we dropped the iteration index for simplicity;
- the intersection $\Omega = S_1 \cap S_2 \cap S_3$ which plays the role of Ω_k in 3PM;

Algorithm 1 Parallel Polyhedral Projection Method (3PM)

```

procedure 3PM( $x_1 \in \mathbb{R}^n$ , closed convex sets  $U_1, \dots, U_m$ )
  if  $x_1 \in U := \bigcap_{i=1}^m U_i$  then
    return  $x_1$ 
  end if
   $k \leftarrow 1$ 
  while  $x_k \notin U$  do
    Compute projections  $P_{U_1}(x_k), \dots, P_{U_m}(x_k)$ 
    Define sets  $S_{ik}$  as in equation (2)
    Define  $\Omega_k$  as in equation (3)
     $x_{k+1} \leftarrow P_{\Omega_k}(x_k)$ 
     $k \leftarrow k + 1$ 
  end while
  return  $x_k$ 
end procedure
  
```

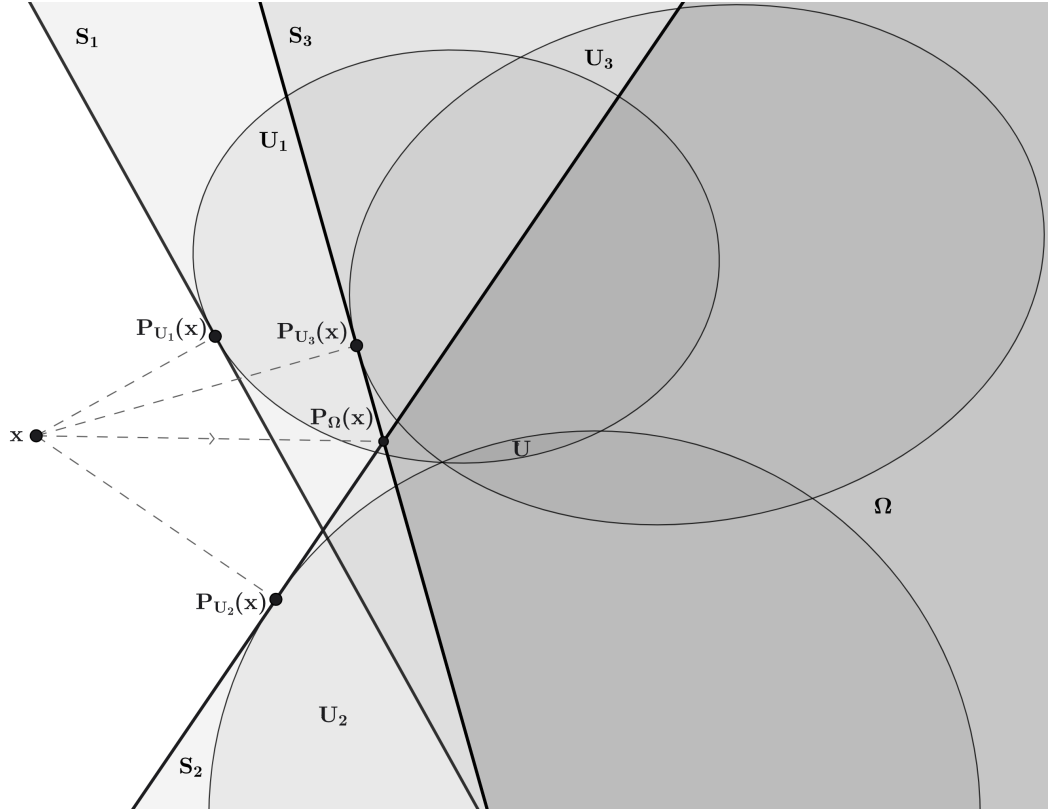


Figure 1: An iteration of 3PM

- the next iterate which is the projection $P_\Omega(x)$ of x onto Ω which is closer (as shown in Lemma 2.2 below) than x (much closer in this example) to any point in the intersection $U := U_1 \cap U_2 \cap U_3$.

It should be noted that if x_k already belongs to U_i then $S_{ik} = \mathbb{R}^n$.

2.2 Convergence analysis

This section is dedicated to the convergence analysis of 3PM.

2.2.1 Convergence proof

We begin by recalling a fundamental property of projections onto closed convex sets, which characterizes the projection as the unique point satisfying a first-order optimality condition. This inequality plays a central role in demonstrating geometric properties of projection-based algorithms such as 3PM.

Proposition 2.1 (Projection characterization) *Let X be a closed nonempty convex set. Then the projection $P_X(z)$ of $z \in \mathbb{R}^n$ onto X satisfies*

$$\langle z - P_X(z), x - P_X(z) \rangle \leq 0, \quad \forall x \in X.$$

Proof: Proof See, e.g., Theorem 3.16 in Bauschke and Combettes [7]. ■

We now turn to the behavior of the sequence (x_k) generated by 3PM. The following lemma shows that this sequence is Fejér monotone with respect to the feasible region U , meaning that the distance from each iterate to any point in U does not increase. This property provides a key tool for establishing convergence results.

Lemma 2.2 (Fejér monotonicity of 3PM) *For any starting point $x_1 \in \mathbb{R}^n$, the sequence (x_k) generated by 3PM satisfies*

$$\|x_k - u\|^2 \geq \|x_k - x_{k+1}\|^2 + \|x_{k+1} - u\|^2 \quad (4)$$

and therefore is Fejér monotone with respect to U , i.e.,

$$\|x_{k+1} - u\| \leq \|x_k - u\|, \quad \forall u \in U. \quad (5)$$

Proof: Proof By Proposition 2.1, we have

$$\langle x_k - x_{k+1}, u - x_{k+1} \rangle \leq 0, \quad \forall u \in \Omega_k. \quad (6)$$

We also have

$$u \in U \Rightarrow u \in U_i, \forall i \Rightarrow u \in \Omega_k, \quad (7)$$

which combined with (6) gives for all $u \in U$,

$$\begin{aligned} \|x_k - u\|^2 &= \|x_k - x_{k+1}\|^2 + \|x_{k+1} - u\|^2 + 2\langle x_k - x_{k+1}, x_{k+1} - u \rangle \\ &\stackrel{(6)}{\geq} \|x_k - x_{k+1}\|^2 + \|x_{k+1} - u\|^2 \end{aligned} \quad (8)$$

and therefore (4), (5) follow. ■

Fejér monotonicity guarantees that the iterates of 3PM never move further from the feasible region. This property, shared by many classical projection schemes, is particularly useful here as it ensures that even approximate polyhedral steps do not destabilize the sequence.

We now derive a consequence of this property.

Proposition 2.3 (Distance bound from Fejér monotonicity) *Let (z_k) be a sequence converging to a point \bar{z} . Suppose that (z_k) is Fejér monotone with respect to a closed, convex set X . Then, for any k , it holds that*

$$\text{dist}(z_k, X) \geq \frac{1}{2} \|z_k - \bar{z}\|. \quad (9)$$

Proof: Proof By Fejér monotonicity, for any $x \in X$ and k ,

$$\|z_\ell - x\| \leq \|z_k - x\| \quad \forall \ell \geq k.$$

Taking the limit as $\ell \rightarrow +\infty$, we get

$$\|\bar{z} - x\| \leq \|z_k - x\|.$$

Substituting $x = P_X(z_k)$ above, we conclude that

$$\|\bar{z} - P_X(z_k)\| \leq \text{dist}(z_k, X).$$

Thus

$$\begin{aligned} \|z_k - \bar{z}\| &\leq \|z_k - P_X(z_k)\| + \|P_X(z_k) - \bar{z}\| \\ &\leq 2 \text{dist}(z_k, X), \end{aligned}$$

yielding (9). ■

The next lemma shows that the distance from each iterate to every individual set U_i vanishes as $k \rightarrow \infty$.

Lemma 2.4 (Vanishing distance to individual sets) *For any starting point $x_1 \in \mathbb{R}^n$, the sequence (x_k) generated by 3PM satisfies*

$$\lim_{k \rightarrow +\infty} \max_{i=1, \dots, m} \text{dist}(x_k, U_i) = 0. \quad (10)$$

Proof: Proof The inclusion $\Omega_k \subset S_{ik}$ for all i implies

$$\|x_k - x_{k+1}\| = \text{dist}(x_k, \Omega_k) \geq \text{dist}(x_k, S_{ik}) = \|x_k - P_{U_i}(x_k)\| = \text{dist}(x_k, U_i).$$

for all i and therefore

$$\|x_k - x_{k+1}\| \geq \max_{i=1, \dots, m} \text{dist}(x_k, U_i),$$

which implies

$$\begin{aligned} \|x_k - u\|^2 &\stackrel{(4)}{\geq} \|x_k - x_{k+1}\|^2 + \|x_{k+1} - u\|^2 \\ &\geq \max_{i=1, \dots, m} \{\text{dist}(x_k, U_i)^2\} + \|x_{k+1} - u\|^2. \end{aligned}$$

Therefore, the series $S_n = \sum_{k=1}^n s_k$ with general term $s_k = \max_{i=1, \dots, m} \{\text{dist}(x_k, U_i)^2\}$ is nondecreasing, bounded by $\|x_1 - u\|^2$ (for any $u \in U$) and therefore converges, implying that s_k converges to 0. ■

Having shown that the iterates become increasingly feasible, we now address the limiting behavior of the 3PM sequence (x_k) .

Lemma 2.5 (Feasibility of accumulation points) *For any starting point $x_1 \in \mathbb{R}^n$, the sequence (x_k) generated by 3PM is bounded and any accumulation point of this sequence belongs to U .*

Proof: Proof Since (x_k) is Fejér monotone with respect to U , we have that x_k is bounded:

$$\|x_k\| \leq \|u\| + \|x_1 - u\|$$

for all $u \in U$. Therefore, it has a convergent subsequence. Let \bar{x} be an accumulation point of (x_k) and let φ such that $x_{\varphi(k)}$ converges to \bar{x} . Then by Lemma 2.4,

$$\lim_{k \rightarrow +\infty} \max_{i=1, \dots, m} \text{dist}(x_{\varphi(k)}, U_i) = 0$$

and by continuity of the distance function, we obtain

$$\max_{i=1, \dots, m} \text{dist}(\bar{x}, U_i) = 0$$

meaning that $\bar{x} \in U$. ■

The following theorem completes the global convergence analysis of 3PM. Building on the Fejér monotonicity, asymptotic feasibility, and boundedness of the sequence, we now establish that the iterates (x_k) converge to a point in the intersection U .

Theorem 2.6 (Global convergence of 3PM) *For any starting point $x_1 \in \mathbb{R}^n$, the sequence (x_k) generated by 3PM converges to a point $\bar{x} \in U$.*

Proof: Proof Since (x_k) is bounded it has accumulation points. We show that there is only one accumulation point. Consider two accumulation points \bar{x} and \bar{y} , which by the previous lemma belong to U , and take subsequences $x_{\varphi(k)}$ and $x_{\psi(k)}$ such that $\bar{x} = \lim_{k \rightarrow +\infty} x_{\varphi(k)}$ and $\bar{y} = \lim_{k \rightarrow +\infty} x_{\psi(k)}$. Then fixing ℓ , for every k sufficiently large, we have by (5) that $\|\bar{x} - x_{\psi(k)}\| \leq \|\bar{x} - x_{\varphi(\ell)}\|$. Taking the limit in the previous inequality, first with respect to $\ell \rightarrow +\infty$ and then with respect to $k \rightarrow +\infty$ we obtain $\|\bar{x} - \bar{y}\| \leq 0$ and therefore $\bar{x} = \bar{y}$, which achieves the proof. ■

2.2.2 Linear convergence of 3PM

This section demonstrates the linear convergence of the 3PM algorithm. To that end, we introduce a standard regularity assumption on the collection of constraint sets, known as the error bound (EB) condition. This condition plays a central role in the convergence theory of projection algorithms, linking the individual distances to the sets U_i with the distance to their intersection.

The error bound condition is also referred to in the literature as linear regularity (Bauschke and Borwein [6, 5]) or subtransversality (Kruger [25]), and it has been widely employed in the analysis of first-order methods for convex feasibility and related problems.

Definition 2.7 (Error bound condition) *Let $\{U_i\}_{i=1}^m$ be closed convex sets in \mathbb{R}^n with nonempty intersection $U := \bigcap_{i=1}^m U_i \neq \emptyset$. We say that the family $\{U_i\}$ satisfies a local error bound condition at $\bar{x} \in U$ if there exist a constant $\omega \in (0, 1)$ and a neighborhood V of \bar{x} such that*

$$\omega \operatorname{dist}(x, U) \leq \max_{1 \leq i \leq m} \operatorname{dist}(x, U_i), \quad \forall x \in V. \quad (11)$$

The error bound condition ensures that no point in a neighborhood of \bar{x} can be simultaneously close to all the sets U_i while being significantly far from their intersection. The constant ω captures the degree of regularity in the configuration of the sets: when the sets meet transversally, this constant is uniformly bounded away from zero. In a geometric sense, ω can be thought of as reflecting the “angle” between the sets at the point of intersection, with sharper angles corresponding to smaller values of ω .

This assumption will serve as a foundation for our convergence rate analysis. In particular, we will show that the EB condition implies linear convergence of the iterates generated by 3PM, and we derive an explicit upper bound on the corresponding asymptotic rate. Furthermore, under additional smoothness and structural assumptions, this analysis is extended to establish superlinear convergence.

We are now in a position to show that the error bound condition implies a linear convergence rate for the 3PM algorithm. The result below shows that, under assumption 11, the sequence (x_k) generated by 3PM converges to a solution at a linear rate, and provides an explicit bound on the asymptotic contraction factor.

Theorem 2.8 (Linear convergence of 3PM) *Let (x_k) be the sequence generated by 3PM for a starting point $x_1 \in \mathbb{R}^n$. Assume that the error bound condition holds for $\{U_i\}_{i=1}^m$ around the limit point \bar{x} of (x_k) . Then (x_k) converges linearly to \bar{x} .*

Proof: Proof By (11), for some $\omega \in (0, 1)$, we have

$$\omega \operatorname{dist}(x_k, U) \leq \max_{i=1, \dots, m} \operatorname{dist}(x_k, U_i) \quad (12)$$

for every sufficiently large k . By Proposition 2.3, we have

$$\operatorname{dist}(x_k, U) \geq \frac{1}{2} \|x_k - \bar{x}\| \quad (13)$$

for any k . Now from (11) with $u = \bar{x}$,

$$\begin{aligned} \|x_k - \bar{x}\|^2 &\geq \max_{i=1, \dots, m} \{\operatorname{dist}(x_k, U_i)^2\} + \|x_{k+1} - \bar{x}\|^2 \\ &\geq \omega^2 \operatorname{dist}(x_k, U)^2 + \|x_{k+1} - \bar{x}\|^2 \\ &\geq \frac{\omega^2}{4} \|x_k - \bar{x}\|^2 + \|x_{k+1} - \bar{x}\|^2. \end{aligned} \quad (14)$$

Rearranging the terms, we arrive at

$$\sqrt{1 - \frac{\omega^2}{4}} \|x_k - \bar{x}\| \geq \|x_{k+1} - \bar{x}\|, \quad (15)$$

proving the linear convergence of 3PM. \blacksquare

The result shows that 3PM not only converges but does so with a guaranteed rate when the constraint sets satisfy a mild regularity condition. In particular, the rate depends explicitly on the error bound constant ω . This analysis also lays the groundwork for understanding regimes where the convergence may be faster than linear, as we explore next.

2.2.3 Superlinear convergence of 3PM

In this section, we establish the superlinear convergence of the 3PM sequence (x_k) under the assumptions stated in Theorem 2.12. In the context of the 3PM algorithm, we denote the projection of x_k onto U_i by $p_{ik} := P_{U_i}(x_k)$, and define the residual vector $d_{ik} := x_k - p_{ik}$.

The assumptions for superlinear convergence include the nonemptiness of the interior of the intersection $U := \bigcap_{i=1}^m U_i$, and the requirement that each boundary ∂U_i is locally a differentiable manifold. These conditions imply that each ∂U_i is a $(n-1)$ -dimensional manifold.

When the boundary of each set U_i is locally smooth, the supporting half-spaces constructed in 3PM can be interpreted as local first-order linearizations of the sets. In this regime, the polyhedron Ω_k formed by these half-spaces approximates the intersection $U = \bigcap_i U_i$ increasingly well as x_k converges to a point in U .

In particular, when the iterates x_k eventually avoid lying too close to the boundary of certain “inactive” sets (e.g., those not containing \bar{x} on their boundary), the supporting half-spaces corresponding to the remaining sets tend to align in a configuration that more accurately captures the local geometry of the feasible region. This selective stabilization has the effect of making the correction step in 3PM increasingly well-directed, exhibiting behavior reminiscent of Newton-like superlinear acceleration.

We begin by presenting Lemmas 2.9 and 2.10, which will be instrumental in the proof of superlinear convergence of 3PM.

Lemma 2.9 (Monotonicity of projection-distance ratio) *Let $X \subset \mathbb{R}^n$ be a nonempty closed convex set, let $x \notin X$ and $p := P_X(x)$. Let any $q \in X$. Then the function*

$$\phi(\mu) := \frac{\text{dist}(p + \mu(x - p), X)}{\|p + \mu(x - p) - q\|}$$

is increasing in $\mu > 0$.

Proof: Proof Since $P_X(p + \mu(x - p)) = p$, we have

$$\phi(\mu) = \frac{\mu \|x - p\|}{\|p - q + \mu(x - p)\|}.$$

Define $a := x - p$ and $b := p - q$. Then

$$\phi(\mu)^2 = \frac{\mu^2 \|a\|^2}{\|b + \mu a\|^2} = \frac{\mu^2 \|a\|^2}{\|b\|^2 + 2\mu \langle a, b \rangle + \mu^2 \|a\|^2} = \frac{\|a\|^2}{\|b\|^2 \frac{1}{\mu^2} + 2\langle a, b \rangle \frac{1}{\mu} + \|a\|^2}.$$

Since $\langle a, b \rangle \geq 0$ by Proposition 2.1, the denominator is increasing in $\frac{1}{\mu}$, then decreasing in μ , hence ϕ is increasing in μ . \blacksquare

As mentioned earlier, the nonemptiness of the interior of U , along with the assumption that the boundaries of U_i are locally differentiable manifolds, implies that these manifolds have dimension $n-1$.

Let $M \subset \mathbb{R}^n$ be any differentiable manifold of dimension $n-1$ and $\bar{z} \in M$. It is well-known that M can be locally written as

$$M = \{z \in \mathbb{R}^n \mid g(z) = 0\}$$

for some function $g : \mathbb{R}^n \rightarrow \mathbb{R}$ of class C^1 with $g(\bar{z}) = 0$ and $\nabla g(\bar{z}) \neq 0$, so that the tangent hyperplane is given by

$$T_M(\bar{z}) := \{z \in \mathbb{R}^n \mid \langle \nabla g(\bar{z}), z - \bar{z} \rangle = 0\}.$$

The following lemma is a vital geometric tool in our analysis. It captures the behavior of sequences approaching a smooth manifold and will play a key role in showing the superlinear convergence of 3PM.

Lemma 2.10 (Tangency limit to manifold) *Let $M \subset \mathbb{R}^n$ be a differentiable manifold of dimension $n-1$ and $\bar{z} \in M$. Suppose that both the sequences $(q_k) \subset M$ and $(z_k) \subset \mathbb{R}^n$ converge to \bar{z} with $z_k \in T_M(q_k)$ and $z_k \neq q_k$. Then*

$$\lim_{k \rightarrow \infty} \frac{\text{dist}(z_k, M)}{\|z_k - q_k\|} = 0.$$

Proof: Proof Take g as described above. Evidently, we only have to consider the case $g(z_k) \neq 0$. For all k large enough, by the fundamental theorem of calculus we have

$$g(z_k) - g(q_k) = g(z_k) = \int_0^1 \langle z_k - q_k, \nabla g(q_k + t(z_k - q_k)) \rangle dt.$$

By assumption, $\langle z_k - q_k, \nabla g(q_k) \rangle = 0$. Hence

$$g(z_k) = \int_0^1 \langle z_k - q_k, \nabla g(q_k + t(z_k - q_k)) - \nabla g(q_k) \rangle dt.$$

Thus

$$|g(z_k)| \leq \int_0^1 \|z_k - q_k\| \cdot \|\nabla g(q_k + t(z_k - q_k)) - \nabla g(q_k)\| dt. \quad (16)$$

Since ∇g is continuous, we have

$$\|\nabla g(q_k + t(z_k - q_k)) - \nabla g(q_k)\| \rightarrow 0$$

as $k \rightarrow +\infty$ uniformly in $t \in [0, 1]$, which implies

$$\lim_{k \rightarrow \infty} \int_0^1 \|\nabla g(q_k + t(z_k - q_k)) - \nabla g(q_k)\| dt = 0. \quad (17)$$

Combining (16) and (17), we obtain

$$\lim_{k \rightarrow \infty} \frac{|g(z_k)|}{\|z_k - q_k\|} = 0. \quad (18)$$

Define

$$\tilde{z}_k := z_k - g(z_k) \frac{2}{\|\nabla g(\bar{z})\|^2} \nabla g(z_k).$$

Then clearly $\tilde{z}_k \rightarrow \bar{z}$. Using the fundamental theorem of calculus again, we get

$$\begin{aligned} g(z_k) - g(\tilde{z}_k) &= \int_0^1 \left\langle \nabla g(\tilde{z}_k + t(z_k - \tilde{z}_k)), g(z_k) \frac{2}{\|\nabla g(\bar{z})\|^2} \nabla g(z_k) \right\rangle dt \\ &= g(z_k) \frac{2}{\|\nabla g(\bar{z})\|^2} \int_0^1 \langle \nabla g(\tilde{z}_k + t(z_k - \tilde{z}_k)), \nabla g(z_k) \rangle dt. \end{aligned}$$

The last integrand converges to $\|\nabla g(\bar{z})\|^2 > 0$, so for all large k we have

$$\int_0^1 \langle \nabla g(\tilde{z}_k + t(z_k - \tilde{z}_k)), \nabla g(z_k) \rangle dt \geq \frac{\|\nabla g(\bar{z})\|^2}{2},$$

which implies

$$\frac{g(z_k) - g(\tilde{z}_k)}{g(z_k)} \geq 1,$$

meaning $g(\tilde{z}_k)$ and $g(z_k)$ have different signs. By continuity of g , there exists $\lambda_k \in [0, 1]$ such that

$$g\left(z_k - \lambda_k g(z_k) \frac{2}{\|\nabla g(\bar{z})\|^2} \nabla g(z_k)\right) = 0, \quad \text{i.e.,} \quad z_k - \lambda_k g(z_k) \frac{2}{\|\nabla g(\bar{z})\|^2} \nabla g(z_k) \in M.$$

Thus

$$\text{dist}(z_k, M) \leq \left\| \lambda_k g(z_k) \frac{2}{\|\nabla g(\bar{z})\|^2} \nabla g(z_k) \right\| \leq |g(z_k)| \frac{2\|\nabla g(z_k)\|}{\|\nabla g(\bar{z})\|^2}.$$

Since $\|\nabla g(z_k)\| \rightarrow \|\nabla g(\bar{z})\| > 0$, we conclude that $\text{dist}(z_k, M) = \mathcal{O}(|g(z_k)|)$. Combining this fact with (18), we obtain:

$$\lim_{k \rightarrow \infty} \frac{\text{dist}(z_k, M)}{\|z_k - q_k\|} = 0. \quad (19)$$

This completes the argument. \blacksquare

The following lemma captures the asymptotic alignment of projection directions near smooth boundaries.

Lemma 2.11 (Alignment of projection directions) *Let $U \subset \mathbb{R}^n$ be closed, convex, with nonempty interior, and suppose ∂U is locally a differentiable manifold. Let $\bar{x} \in \partial U$, and let $x_k \notin U$ with $x_k \rightarrow \bar{x}$. Define $p_k := P_U(x_k)$. Then*

$$\lim_{k \rightarrow \infty} \cos \angle(x_k - p_k, x_{k+1} - p_{k+1}) = 1.$$

Proof: Proof Since $x_k \notin U$, we have $p_k \in \partial U$ and $x_k - p_k \in N_U(p_k)$, so:

$$\frac{x_k - p_k}{\|x_k - p_k\|} \in N_U(p_k) \cap \mathbb{S}^{n-1}.$$

By local differentiability, there exists an open ball B containing \bar{x} and a function $g \in C^1(B)$ such that:

$$U \cap B = \{x \in B : g(x) \leq 0\}, \quad \partial U \cap B = \{x \in B : g(x) = 0\}, \quad \nabla g(x) \neq 0 \text{ on } B.$$

For all sufficiently large k , $p_k \in B$, so:

$$N_U(p_k) = \mathbb{R}_+ \nabla g(p_k) \quad \text{and} \quad \frac{x_k - p_k}{\|x_k - p_k\|} = \frac{\nabla g(p_k)}{\|\nabla g(p_k)\|}.$$

Since ∇g is continuous and $p_k \rightarrow \bar{x}$, we conclude:

$$\frac{\nabla g(p_k)}{\|\nabla g(p_k)\|} \rightarrow \frac{\nabla g(\bar{x})}{\|\nabla g(\bar{x})\|} = n(\bar{x}),$$

where $n(\bar{x})$ is the outward unit normal to ∂U at \bar{x} . Thus it becomes evident that

$$\cos \angle(x_k - p_k, x_{k+1} - p_{k+1}) = \left\langle \frac{x_k - p_k}{\|x_k - p_k\|}, \frac{x_{k+1} - p_{k+1}}{\|x_{k+1} - p_{k+1}\|} \right\rangle = \left\langle \frac{\nabla g(p_k)}{\|\nabla g(p_k)\|}, \frac{\nabla g(p_{k+1})}{\|\nabla g(p_{k+1})\|} \right\rangle \rightarrow 1.$$

Finally, we are ready to formalize a result that has been discussed throughout the paper: under a geometric condition, the convergence of 3PM improves beyond linear. Specifically, if the iterates eventually avoid the boundary sets active at the limit point, the polyhedral correction becomes increasingly accurate, yielding superlinear convergence. \blacksquare

Theorem 2.12 (Superlinear convergence of 3PM) *Assume that $\text{int}(U) \neq \emptyset$ and each boundary ∂U_i is locally a differentiable manifold. Let (x_k) be the sequence generated by 3PM for a starting point $x_1 \in \mathbb{R}^n$, which converges to \bar{x} . Define $I = \{i \mid \bar{x} \notin \text{int}(U_i)\}$. Assume that $x_k \notin \bigcup_{i \in I} U_i$ for all k large enough. Assume also that the error bound condition holds for $\{U_i\}_{i=1}^m$ around the limit point \bar{x} of (x_k) . Then x_k converges to \bar{x} superlinearly.*

Proof: Proof We have $x_k \in \bigcap_{i \notin I} U_i$ for all k large enough. From this point on, the sequence is defined only by $\{U_i \mid i \in I\}$. Moreover, it is clear that $\bar{x} \in \bigcap_{i \in I} \partial U_i$. For each $i \in I$, Lemma 2.11 implies

$$\cos \angle(d_{ik+1}, d_{ik}) \rightarrow 1. \quad (20)$$

Choose i satisfying $\|d_{ik+1}\| = \max_{j \in I} \|d_{j,k+1}\|$. Let

$$y_k := x_{k+1} + \mu_k d_{ik+1}, \quad \text{where} \quad \mu_k := \frac{\langle p_{ik} - x_{k+1}, d_{ik} \rangle}{\langle d_{ik+1}, d_{ik} \rangle}.$$

Then for all k large enough, $\mu_k \geq 0$ and

$$\langle y_k - p_{ik}, d_{ik} \rangle = \langle x_{k+1} - p_{ik} + \mu_k d_{ik+1}, d_{ik} \rangle = -\langle p_{ik} - x_{k+1}, d_{ik} \rangle + \mu_k \langle d_{ik+1}, d_{ik} \rangle = 0.$$

That means $y_k \in \partial S_{ik}$. Notice that

$$\begin{aligned} \|y_k - x_{k+1}\| &= \mu_k \|d_{ik+1}\| \\ &= \frac{\langle p_{ik} - x_{k+1}, d_{ik} \rangle}{\langle d_{ik+1}, d_{ik} \rangle} \cdot \|d_{ik+1}\| \\ &= \frac{\|p_{ik} - x_{k+1}\| \cdot \|d_{ik}\| \cdot \cos \angle(p_{ik} - x_{k+1}, d_{ik})}{\|d_{ik+1}\| \cdot \|d_{ik}\| \cdot \cos \angle(d_{ik+1}, d_{ik})} \cdot \|d_{ik+1}\| \\ &= \|p_{ik} - x_{k+1}\| \cdot \frac{\cos \angle(p_{ik} - x_{k+1}, d_{ik})}{\cos \angle(d_{ik+1}, d_{ik})}. \end{aligned}$$

Result (20), together with the convergences $\|p_{ik} - x_{k+1}\| \rightarrow 0$ and $x_{k+1} \rightarrow \bar{x}$, yields $y_k \rightarrow \bar{x}$. Clearly we also have $p_{ik} \rightarrow \bar{x}$. From the tangency of ∂S_{ik} to U_i at p_{ik} (see, e.g., Theorems 23.2 and 25.1 in Rockafellar 1997 [31]) and the fact that $y_k \in \partial S_{ik}$, we can apply Lemma 2.10 to conclude that

$$\lim_{k \rightarrow \infty} \frac{\text{dist}(y_k, U_i)}{\|y_k - p_{ik}\|} = 0. \quad (21)$$

Since $\mu_k \geq 0$, by Lemma 2.9, we get

$$\frac{\text{dist}(x_{k+1}, U_i)}{\|x_{k+1} - p_{ik}\|} \leq \frac{\text{dist}(y_k, U_i)}{\|y_k - p_{ik}\|}. \quad (22)$$

Meanwhile, $U \subset \Omega_k$ forces $\text{dist}(x_k, U) \geq \|x_k - x_{k+1}\|$ and, by $x_{k+1} \in S_{ik}$, Proposition 2.1 means that

$$\|x_k - x_{k+1}\|^2 \geq \|x_{k+1} - p_{ik}\|^2 + \|x_k - p_{ik}\|^2,$$

hence $\text{dist}(x_k, U) \geq \|x_{k+1} - p_{ik}\|$. So

$$\frac{\text{dist}(x_{k+1}, U_i)}{\text{dist}(x_k, U)} \leq \frac{\text{dist}(x_{k+1}, U_i)}{\|x_{k+1} - p_{ik}\|}. \quad (23)$$

Now the error bound condition, implied by $\text{int}(U) \neq \emptyset$, yields

$$\frac{\text{dist}(x_{k+1}, U)}{\text{dist}(x_k, U)} \leq \frac{1}{\omega} \cdot \frac{\max_j \{\text{dist}(x_{k+1}, U_j)\}}{\text{dist}(x_k, U)} = \frac{1}{\omega} \cdot \frac{\text{dist}(x_{k+1}, U_i)}{\text{dist}(x_k, U)}. \quad (24)$$

Using Proposition 2.3 and the inequality $\text{dist}(x_k, U) \leq \|x_k - \bar{x}\|$, we get

$$\frac{\|x_{k+1} - \bar{x}\|}{\|x_k - \bar{x}\|} \leq 2 \cdot \frac{\text{dist}(x_{k+1}, U)}{\text{dist}(x_k, U)}. \quad (25)$$

Combining (22), (23), (24) and (25), it follows that

$$\frac{\|x_{k+1} - \bar{x}\|}{\|x_k - \bar{x}\|} \leq \frac{2}{\omega} \cdot \frac{\text{dist}(y_k, U_i)}{\|y_k - p_{ik}\|}.$$

Finally, plugging (21) in the above inequality, we arrive at

$$\lim_{k \rightarrow \infty} \frac{\|x_{k+1} - \bar{x}\|}{\|x_k - \bar{x}\|} = 0,$$

demonstrating the desired superlinear convergence. ■

2.3 P-CRM and MAP as special cases of 3PM

In this section, we explore how 3PM relates to two classical projection methods, highlighting shared geometric principles and algorithmic structures. These connections help situate 3PM within the broader landscape of projection-based algorithms and provide insights into its potential strengths.

We begin by showing that 3PM recovers the Parallel Circumcentered-Reflection Method (P-CRM) from Barros et al. [4] when the second-phase projection lands exactly on the boundaries of all supporting half-spaces. To do so, we recall the notion of a circumcenter, which plays a central role in the formulation of CRM.

Definition 2.13 (Circumcenter) *Let $\{z_0, z_1, \dots, z_m\} \subset \mathbb{R}^n$. The circumcenter of this set is the point $c \in \text{aff}\{z_0, z_1, \dots, z_m\}$ such that $\|c - z_0\| = \|c - z_1\| = \dots = \|c - z_m\|$.*

This point c is equidistant from all given reference points and lies within their affine span. It exists and is unique, for example, if z_0, z_1, \dots, z_m are affinely independent, as shown by Bauschke et al. [8]. In the context of CRM, the points z_i are obtained by reflecting the current iterate z_k across each set U_i . Specifically, the Parallel CRM iteration is given by $T_{\text{P-CRM}}(z) := \text{circ}(z, R_{U_1}(z), \dots, R_{U_m}(z))$, where each reflection is defined as $R_{U_i}(z) := 2P_{U_i}(z) - z$.

When the projection step in 3PM lands on the boundary of all supporting half-spaces, i.e., when $x_{k+1} \in \partial S_{ik}$ for all i , the update coincides with that of Parallel CRM. In this case, the intersection of supporting half-spaces used in 3PM aligns with the affine geometry of the reflected points in P-CRM, and both methods yield the same next iterate.

Proposition 2.14 (P-CRM as a special case of 3PM) *Suppose that, at iteration k , the projection onto the polyhedron Ω_k in 3PM satisfies $x_{k+1} \in \partial S_{ik}$ for all $i = 1, \dots, m$; that is, all supporting half-spaces used to define Ω_k are active at the projection step. Then, the 3PM update coincides with the P-CRM update of x_k with respect to the family $\{U_i\}_{i=1}^m$. In other words,*

$$x_{k+1} = \text{circ}(x_k, R_{U_1}(x_k), \dots, R_{U_m}(x_k)).$$

Proof: Proof Let us denote $H_{ik} = \partial S_{ik}$ and $W_k = \text{aff}(x_k, p_{1k}, \dots, p_{mk})$.

Since $H := \bigcap_i H_{ik}$ is a convex subset of $\bigcap_i S_{ik}$ containing x_{k+1} , we conclude that $x_{k+1} = P_H(x_k)$. Now, since H and H_{ik} are subspaces with $H \subset H_{ik}$, we have

$$x_{k+1} = P_H(x_k) = P_H(p_{ik}) \quad \text{for all } i.$$

We deduce that for every $w \in W_k$, we also have $x_{k+1} = P_H(w)$. In particular, $x_{k+1} = P_H(P_{W_k}(x_{k+1}))$, which implies that

$$x_{k+1} - P_{W_k}(x_{k+1}) \in H^\perp. \quad (26)$$

But from $x_k, p_{ik} \in W_k$, it follows that

$$x_{k+1} - P_{W_k}(x_{k+1}) \in (\text{span}\{x_k - p_{ik}\})^\perp = H_{ik} \quad \forall i.$$

Therefore,

$$x_{k+1} - P_{W_k}(x_{k+1}) \in \bigcap_i H_{ik} = H. \quad (27)$$

Uniting (26) and (27), we conclude that $x_{k+1} - P_{W_k}(x_{k+1}) = 0$, that is

$$x_{k+1} \in W_k. \quad (28)$$

Let us now consider the reflections of x_k across each set U_i , denoted by $r_{ik} := 2p_{ik} - x_k$. Since by assumption, $\langle x_k - p_{ik}, x_{k+1} - p_{ik} \rangle = 0$, we know that the triangle with vertices x_k , p_{ik} , and x_{k+1} is right-angled at p_{ik} . Now, by the Pythagorean theorem, we compute the squared distance from x_{k+1} to the reflection point r_{ik} :

$$\|x_{k+1} - r_{ik}\|^2 = \|x_{k+1} - p_{ik}\|^2 + \|x_k - p_{ik}\|^2.$$

Similarly, the distance from x_k to x_{k+1} is:

$$\|x_k - x_{k+1}\|^2 = \|x_{k+1} - p_{ik}\|^2 + \|x_k - p_{ik}\|^2.$$

So we conclude:

$$\|x_{k+1} - r_{ik}\| = \|x_k - x_{k+1}\|, \quad \forall i. \quad (29)$$

Properties (28) and (29) show that $x_{k+1} = T_{\text{P-CRM}}(x_k)$. \blacksquare

If the condition in the proposition above holds throughout the iterations of 3PM, and assuming $\text{int}(U) \neq \emptyset$ with each boundary ∂U_i locally a differentiable manifold, then Theorem 2.12 guarantees superlinear convergence. This behavior is reminiscent of the centralized Circumcentered-Reflection Method from Behling et al. [14], which also attains superlinear convergence under similar assumptions.

We also recover the classical Method of Alternating Projections (MAP) as a limiting case of 3PM when the number of sets is two and the iterates remain on one of the sets:

Proposition 2.15 (MAP as a special case of 3PM) *If $m = 2$ and there exists an iteration k such that $x_k \in U_1 \cup U_2$, then 3PM coincides with MAP from that iteration onward.*

Proof: Proof Suppose without loss of generality that $x_k \in U_1$. Then the projection $p_{1k} = x_k$, and $p_{2k} = P_{U_2}(x_k)$. The supporting half-spaces reduce to $S_{1k} = \mathbb{R}^n$ and S_{2k} , a half-space orthogonal to the segment from x_k to p_{2k} . The polyhedral projection step in 3PM then becomes $x_{k+1} = P_{S_{2k}}(x_k) = P_{U_2}(x_k)$. In the next iteration, we reverse roles and project back onto U_1 , so 3PM cycles between U_1 and U_2 , exactly replicating MAP. \blacksquare

These connections illustrate the versatility of 3PM: it interpolates between and generalizes important existing projection schemes while introducing a novel polyhedral correction step that can improve convergence, especially when $m > 2$.

3 Approximate Parallel Polyhedral Projection Method for Convex Feasibility problems (A3PM)

3.1 A3PM method

In this section, we introduce the inexact extension of 3PM, called A3PM, which allows for approximate projections in both phases of the method. Exact projections are often computationally expensive or unavailable in closed form. A3PM addresses this challenge by permitting controlled inexactness in the computation of projections while still preserving convergence under mild conditions.

The algorithm starts from an arbitrary point $x_1 = x$, and at each iteration $k \geq 1$, given x_k , it computes approximate projections $\hat{P}_{U_i}(x_k, \varepsilon)$ of x_k onto each set U_i , with a uniform accuracy parameter $0 \leq \varepsilon < 1$. The approximate projection operator $\hat{P}_{U_i}(\cdot, \varepsilon)$ is defined as follows:

Definition 3.1 (Approximate projection operator) *Let X be a closed nonempty convex set and let $\varepsilon \in [0, 1)$. An approximate projection $\hat{P}_X(x, \varepsilon)$ of x onto X with accuracy ε is any point \hat{x} satisfying the two properties (i) and (ii) below:*

- (i) $\text{dist}(\hat{x}, X) \leq \varepsilon \text{dist}(x, X)$;
- (ii) X is contained in the set $\left\{ z : \langle z - \hat{x}, x - \hat{x} \rangle \leq 0 \right\}$.

When $\varepsilon = 0$, we get the exact projection $\hat{P}_X(x, 0) = P_X(x)$ and for $\varepsilon = 0$ A3PM becomes 3PM.

The Approximate Parallel Polyhedral Projection Method (A3PM) for Convex Feasibility problems replaces in 3PM the projections by approximate projections. More precisely, A3PM is given below in Algorithm 2.

A more general variant of A3PM allows the accuracy parameter to vary across iterations, using a sequence (ε_k) in $[0, 1)$ instead of a fixed value ε . The corresponding method is given in Algorithm 3 below.

Figure 2 illustrates the computation of an iteration of A3PM for 3 sets U_1 , U_2 , and U_3 in \mathbb{R}^2 . In this figure we represent:

Algorithm 2 Approximate Parallel Polyhedral Projection Method (A3PM)

procedure A3PM($x_1 \in \mathbb{R}^n$, sets U_1, \dots, U_m , tolerance $\varepsilon \in [0, 1)$)
 $k \leftarrow 1$
 while stopping criterion not met **do**
 Compute approximate projections:
 $\hat{P}_{U_1}(x_k, \varepsilon), \dots, \hat{P}_{U_m}(x_k, \varepsilon)$
 Define sets \hat{S}_{ik} by:
 $\hat{S}_{ik} := \left\{ z : \langle x_k - \hat{P}_{U_i}(x_k, \varepsilon), z - \hat{P}_{U_i}(x_k, \varepsilon) \rangle \leq 0 \right\}$
 Define $\hat{\Omega}_k := \bigcap_{i=1}^m \hat{S}_{ik}$
 Compute $\hat{P}_{\hat{\Omega}_k}(x_k, \varepsilon)$
 Update $x_{k+1} \leftarrow \hat{P}_{\hat{\Omega}_k}(x_k, \varepsilon)$
 $k \leftarrow k + 1$
 end while
 return x_k
end procedure

Algorithm 3 A3PM with Dynamic Accuracy

procedure A3PM-DYNAMIC($x_1 \in \mathbb{R}^n$, sets U_1, \dots, U_m , sequence $(\varepsilon_k) \subset [0, 1)$)
 $k \leftarrow 1$
 while stopping criterion not met **do**
 Compute approximate projections:
 $\hat{P}_{U_1}(x_k, \varepsilon_k), \dots, \hat{P}_{U_m}(x_k, \varepsilon_k)$
 Define sets \hat{S}_{ik} by:
 $\hat{S}_{ik} := \left\{ z : \langle x_k - \hat{P}_{U_i}(x_k, \varepsilon_k), z - \hat{P}_{U_i}(x_k, \varepsilon_k) \rangle \leq 0 \right\}$
 Define $\hat{\Omega}_k := \bigcap_{i=1}^m \hat{S}_{ik}$
 Compute $\hat{P}_{\hat{\Omega}_k}(x_k, \varepsilon_k)$
 Update $x_{k+1} \leftarrow \hat{P}_{\hat{\Omega}_k}(x_k, \varepsilon_k)$
 $k \leftarrow k + 1$
 end while
 return x_k
end procedure

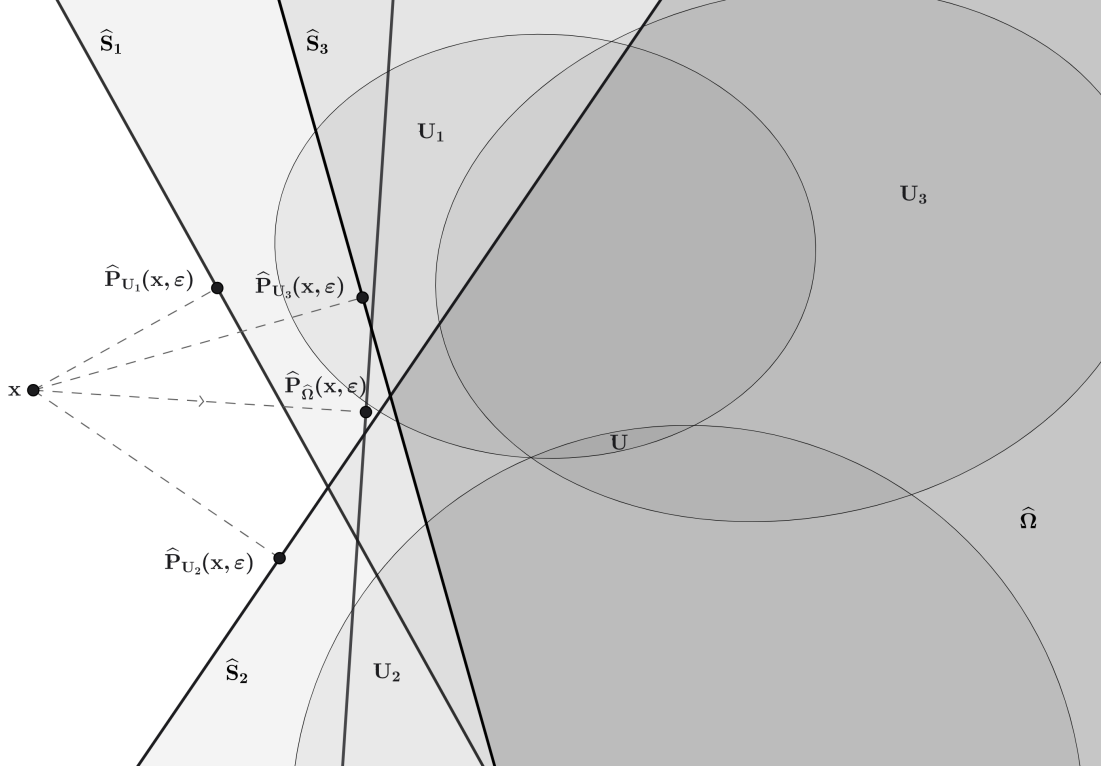


Figure 2: An iteration of A3PM

- convex sets U_1 , U_2 , and U_3 and their intersection U ;
- an arbitrary initial point x ;
- the approximate projections $\hat{P}_{U_1}(x, \varepsilon)$, $\hat{P}_{U_2}(x, \varepsilon)$, and $\hat{P}_{U_3}(x, \varepsilon)$ of x onto respectively U_1 , U_2 , and U_3 ;
- half-spaces \hat{S}_1 , \hat{S}_2 , and \hat{S}_3 which play the role of half-spaces \hat{S}_{ik} in A3PM; we dropped the iteration index for simplicity;
- the intersection $\hat{\Omega} = \hat{S}_1 \cap \hat{S}_2 \cap \hat{S}_3$ which plays the role of $\hat{\Omega}_k$ in A3PM;
- the next iterate which is the approximate projection $\hat{P}_{\hat{\Omega}}(x, \varepsilon)$ of x onto $\hat{\Omega}$.

3.2 Convergence analysis

In this section, we study the convergence properties of A3PM in its most general form, where the accuracy level of the approximate projections may vary across iterations. That is, we consider a sequence of accuracies $(\varepsilon_k) \subset [0, 1)$ used in each step of the algorithm. We assume throughout this section that $\sup_k \varepsilon_k < 1$.

This dynamic formulation includes, as a special case, the fixed-accuracy variant of A3PM where a single value $\varepsilon \in [0, 1)$ is used at every iteration. Thus, the results below apply to both forms of the algorithm.

We begin with an elementary property of the approximate projection:

Lemma 3.2 (Bound on step size of approximate projection) *For any set X and point x , let $\hat{P}_X(x, \varepsilon)$ be an approximate projection of x onto X . Then*

$$\|x - \hat{P}_X(x, \varepsilon)\| \geq (1 - \varepsilon) \text{dist}(x, X). \quad (30)$$

Proof: Proof Setting $\hat{x} = \hat{P}_X(x, \varepsilon)$, by definition of the approximate projection,

$$\text{dist}(\hat{x}, X) = \|\hat{x} - P_X(\hat{x})\| \leq \varepsilon \text{dist}(x, X).$$

Hence,

$$\begin{aligned} \|x - \hat{x}\| &\geq \|x - P_X(\hat{x})\| - \|\hat{x} - P_X(\hat{x})\| \\ &\geq \text{dist}(x, X) - \varepsilon \text{dist}(x, X) \\ &= (1 - \varepsilon) \text{dist}(x, X). \end{aligned}$$

■

The following lemma is for A3PM the analogue of Lemma 2.4 for 3PM:

Lemma 3.3 (Vanishing setwise distance for A3PM) *For any starting point $x_1 \in \mathbb{R}^n$, the sequence (x_k) generated by A3PM satisfies*

$$\lim_{k \rightarrow +\infty} \max_{i=1, \dots, m} \text{dist}(x_k, U_i) = 0. \quad (31)$$

Proof: Proof Lemma 3.2 with $x = x_k$, $\varepsilon = \varepsilon_k$, and $X = \hat{\Omega}_k$, gives

$$\|x_k - x_{k+1}\| \geq (1 - \varepsilon_k) \text{dist}(x_k, \hat{\Omega}_k). \quad (32)$$

Next, notice that

$$\hat{\Omega}_k \subset \hat{S}_{ik} \implies \text{dist}(x_k, \hat{\Omega}_k) \geq \text{dist}(x_k, \hat{S}_{ik}) = \|x_k - \hat{P}_{U_i}(x_k, \varepsilon_k)\|$$

and using Lemma 3.2 with $x = x_k$, $\varepsilon = \varepsilon_k$, and $X = U_i$, we deduce for all i :

$$\text{dist}(x_k, \hat{\Omega}_k) \geq (1 - \varepsilon_k) \text{dist}(x_k, U_i). \quad (33)$$

Relations (32) and (33) give

$$\|x_k - x_{k+1}\| \geq (1 - \varepsilon_k)^2 \max_{i=1, \dots, m} \text{dist}(x_k, U_i). \quad (34)$$

We have, by definition of x_{k+1} and of the approximate projection, that for all $u \in \hat{\Omega}_k$

$$\langle u - x_{k+1}, x_k - x_{k+1} \rangle \leq 0 \quad (35)$$

and since $U_i \subset \hat{S}_{ik}$, $U \subset \hat{\Omega}_k$, we also have for every $u \in U$ that (35) holds. It follows that for every $u \in U$,

$$\begin{aligned} \|u - x_k\|^2 &= \|x_k - x_{k+1}\|^2 + \|u - x_{k+1}\|^2 + 2\langle u - x_{k+1}, x_k - x_{k+1} \rangle \\ &\geq (1 - \varepsilon_k)^4 \max_{i=1, \dots, m} \{\text{dist}(x_k, U_i)^2\} + \|u - x_{k+1}\|^2 \\ &\geq (1 - \sup \varepsilon_k)^4 \max_{i=1, \dots, m} \{\text{dist}(x_k, U_i)^2\} + \|u - x_{k+1}\|^2. \end{aligned} \quad (36)$$

We conclude that $(\|u - x_k\|)_k$ is decreasing and nonnegative, so it is convergent. Then, since $\sup \varepsilon_k < 1$, we obtain (31). ■

The following theorem proves the convergence of A3PM.

Theorem 3.4 (Global convergence of A3PM) *For any starting point $x_1 \in \mathbb{R}^n$, the sequence (x_k) generated by A3PM converges to a point $\bar{x} \in U$.*

Proof: Proof Recall that Lemma 3.3 for A3PM is the analogue of Lemma 2.4 for 3PM. Also observe that Lemma 2.5 still holds for A3PM since the relation $\|x_{k+1} - u\| \leq \|x_k - u\|$ for all $u \in U$ on which it is based also holds. We can then prove Theorem 3.4 similarly to Theorem 2.6. ■

We conclude the analysis of A3PM by showing that linear convergence is also retained under the error bound condition.

Theorem 3.5 (Linear convergence of A3PM) *Let (x_k) be the sequence generated by A3PM for a starting point $x_1 \in \mathbb{R}^n$. Assume that the error bound condition (11) holds for $\{U_i\}_{i=1}^m$ around the limit point \bar{x} of (x_k) . Then (x_k) converges linearly to \bar{x} .*

Proof: Proof By (11), for some $\omega \in (0, 1)$, we have

$$\omega \text{dist}(x_k, U) \leq \max_{i=1, \dots, m} \text{dist}(x_k, U_i) \quad (37)$$

for every sufficiently large k . Notice that (x_k) is Fejér monotone with respect to U by (36). Hence we can apply Proposition 2.3 to conclude that

$$\text{dist}(x_k, U) \geq \frac{1}{2} \|x_k - \bar{x}\| \quad (38)$$

for any k . Now from (36) written with $u = \bar{x}$,

$$\begin{aligned} \|x_k - \bar{x}\|^2 &\geq (1 - \varepsilon_k)^4 \max_{i=1, \dots, m} \{\text{dist}(x_k, U_i)^2\} + \|x_{k+1} - \bar{x}\|^2 \\ &\geq (1 - \varepsilon_k)^4 \omega^2 \text{dist}(x_k, U)^2 + \|x_{k+1} - \bar{x}\|^2 \\ &\geq (1 - \varepsilon_k)^4 \frac{\omega^2}{4} \|x_k - \bar{x}\|^2 + \|x_{k+1} - \bar{x}\|^2 \\ &\geq (1 - \sup \varepsilon_k)^4 \frac{\omega^2}{4} \|x_k - \bar{x}\|^2 + \|x_{k+1} - \bar{x}\|^2. \end{aligned} \quad (39)$$

Rearranging the terms, we arrive at

$$\sqrt{1 - (1 - \sup \varepsilon_k)^4 \frac{\omega^2}{4}} \|x_k - \bar{x}\| \geq \|x_{k+1} - \bar{x}\|, \quad (40)$$

establishing the linear convergence of A3PM. ■

4 Numerical experiments

To see how well the proposed 3PM and A3PM methods perform in practice, we consider the problem of finding a point in the intersection of m ellipsoids U_1, \dots, U_m in \mathbb{R}^n where each ellipsoid U_i is centered at $y_i \in \mathbb{R}^n$ and is given by

$$U_i = \{y \in \mathbb{R}^n : (y - y_i)^T Q_i (y - y_i) \leq \eta_i^2\} \quad (41)$$

for some positive scalars η_i and positive definite matrices Q_i . We generate the centers y_i randomly, and define Q_i of the form $Q_i = A_i A_i^T + \lambda_i I_n$ where matrices A_i and positive λ_i are also generated randomly. In that manner, matrices Q_i are positive definite, as desired. We also choose η_i sufficiently large so that the intersection of sets U_i contains the unit ball $B = \{x : \|x\|_2 \leq 1\}$, namely

$$\eta_i \geq (1 + \|y_i\|_2) \sqrt{\|Q_i\|_2} \quad (42)$$

for all i (in particular, the intersection is nonempty). Indeed, if (42) is satisfied and x belongs to B , then

$$(x - y_i)^T Q_i (x - y_i) \leq \|x - y_i\|_2^2 \|Q_i\|_2 \leq (1 + \|y_i\|_2)^2 \|Q_i\|_2 \leq \eta_i^2$$

and therefore $x \in U_i$. Initial points x_0 are also generated randomly.

For convenience, in what follows, for $i = 1, \dots, m$, we define function $g_i(y) = (y - y_i)^T Q_i (y - y_i) - \eta_i^2$ which is differentiable with gradient $g'_i(y) = 2Q_i(y - y_i)$. We compare 3PM and A3PM with four competing methods: cyclic projections, Cimmino's method, Successive Centralized CRM (SCCRM) from Behling et al. [14], and CRM in the product space (denoted by CRM in what follows) from Behling et al. [16].

We now briefly describe the computations of the iterations of these methods.

For the details of A3PM, we will use the approximate projection proposed by Fukushima [22] that we start recalling. More precisely, the following proposition defines an approximate projector over a closed convex set, which, without loss of generality, can be written under the form $\{x \in \mathbb{R}^n : g(x) \leq 0\}$ for $g : \mathbb{R}^n \rightarrow \mathbb{R}$.

Proposition 4.1 Consider the closed convex set $K := \{x \mid g(x) \leq 0\}$ where $g(x) : \mathbb{R}^n \rightarrow \mathbb{R}$ is convex. Suppose that there exists \hat{x} such that $g(\hat{x}) < 0$ (Slater condition). Let g' satisfy $g'(x) \in \partial g(x)$ for any x . Moreover, let

$$\tilde{p}(x) := \operatorname{argmin}_y \|y - x\| \quad \text{s.t.} \quad g(x) + g'(x)^\top (y - x) \leq 0.$$

Then

$$\tilde{p}(x) = \begin{cases} x, & \text{if } g(x) \leq 0 \\ x - \frac{g(x)}{\|g'(x)\|^2} g'(x), & \text{otherwise,} \end{cases}$$

and \tilde{p} is an ε -approximate projector over K for some $0 < \varepsilon < 1$.

We are now ready to provide the details of the computation of all methods.

3PM. At iteration k , given x_k , 3PM computes

$$p_{ik} = \begin{cases} \operatorname{argmin}_{y \in \mathbb{R}^n} \frac{1}{2} \|y - x_k\|_2^2 \\ g_i(y) \leq 0, \end{cases} \quad (43)$$

for $i = 1, \dots, m$ and then sets

$$x_{k+1} = \begin{cases} \operatorname{argmin}_{y \in \mathbb{R}^n} \frac{1}{2} \|y - x_k\|_2^2 \\ (x_k - p_{ik})^\top (y - p_{ik}) \leq 0, \quad i = 1, \dots, m. \end{cases} \quad (44)$$

A3PM. We first compute the approximate projections over the ellipsoids using Proposition 4.1. At iteration k , for $i = 1, \dots, m$, if $g_i(x_k) \leq 0$, we compute

$$p_{ik} = x_k,$$

otherwise, we compute

$$p_{ik} = x_k - \frac{g_i(x_k)}{\|g'_i(x_k)\|_2^2} g'_i(x_k).$$

For the final step of A3PM, we look for an approximate projection of x_k onto the closed convex set $K = \{x : h(x) \leq 0\}$ where $h(x) = \max_{i=1, \dots, m} h_i(x)$ for

$$h_i(x) = \langle x_k - p_{ik}, x - p_{ik} \rangle.$$

A subgradient $h'(x_k)$ of h at x_k is given by

$$h'(x_k) = x_k - p_{i_k k}$$

where index i_k is any index i satisfying $h(x_k) = h_i(x_k)$.

With this notation, if $h(x_k) \leq 0$ then the approximate projection is $x_{k+1} = x_k$ otherwise it is given by

$$x_{k+1} = x_k - \frac{h(x_k)}{\|h'(x_k)\|_2^2} h'(x_k).$$

Though the letter P in 3PM and A3PM stands for Parallel and refers to the fact that the projections can be computed in parallel in these methods, we can also implement non-parallel variants of these methods where projections are computed sequentially. In what follows, we denote by 3PM \parallel and A3PM \parallel , respectively. implementations while the parallel implementations are denoted by 3PM \parallel and A3PM \parallel , respectively.

Cyclic projections. For iteration k , given x_k , set $x = x_k$ and for $i = 1, \dots, m$, perform iteratively

$$x \leftarrow \begin{cases} \operatorname{argmin}_{y \in \mathbb{R}^n} \frac{1}{2} \|y - x\|_2^2 \\ g_i(y) \leq 0. \end{cases} \quad (45)$$

After these m updates (projections), do $x_{k+1} \leftarrow x$, $k \leftarrow k + 1$.

Cimmino's method. At iteration k , do

$$x_{k+1} \leftarrow \frac{1}{m} \sum_{i=1}^m \left\{ \begin{array}{l} \operatorname{argmin}_{y \in \mathbb{R}^n} \frac{1}{2} \|y - x_k\|_2^2 \\ g_i(y) \leq 0, \end{array} \right.$$

and set $k \leftarrow k + 1$. For Cimmino's method, we can also consider a parallel implementation which computes in parallel the m projections. We denote by Cimmino \parallel the corresponding implementation.

Successive Centralized CRM (SCCRM). We now recall the SCCRM method described in Behling et al. [30]. We first define the alternating projection operator $Z_{A,B} : \mathbb{R}^n \rightarrow \mathbb{R}^n$ given by

$$Z_{A,B} = P_A \circ P_B$$

as well as the simultaneous projection operator $\tilde{Z}_{A,B} : \mathbb{R}^n \rightarrow \mathbb{R}^n$ given by

$$\tilde{Z}_{A,B} = \frac{1}{2} [P_A + P_B].$$

We also define the operator $\bar{Z}_{A,B} : \mathbb{R}^n \rightarrow \mathbb{R}^n$ by

$$\bar{Z}_{A,B} = \tilde{Z}_{A,B} \circ Z_{A,B}$$

and the operator

$$\mathcal{C}_{A,B}(z) = \operatorname{circ}(z, R_A(z), R_B(z)).$$

where $R_A = 2P_A - I$, $R_B = 2P_B - I$, $\operatorname{circ}(a, b, c)$ is the circumcenter of points a, b , and c . With this notation, we finally define the operator $T_{A,B} : \mathbb{R}^n \rightarrow \mathbb{R}^n$ by

$$T_{A,B}(x) = \mathcal{C}_{A,B}(\bar{Z}_{A,B}(x)).$$

The SCCRM method for the convex feasibility problem computes

$$x_{k+1} = T_{U_{r(k)} U_{\ell(k)}}(x_k)$$

where the sequences $\{\ell(k)\}, \{r(k)\}$ determining which sets are used at k th iteration are called control sequences. We use the following control sequences $\ell(k) = 1, 2, 3, \dots, m-1, m, 1, 2, \dots$, and $r(k) = 2, 3, 4, \dots, m-1, m, 1, 2, 3, \dots$. To complete the description of SCCRM, we now explain how to compute the circumcenter of a given set of points. Given $m+1$ points $x_0, x_1, x_2, \dots, x_m \in \mathbb{R}^n$, their circumcenter, denoted by $\operatorname{circ}(x_0, x_1, x_2, \dots, x_m)$, is defined as the unique point that lies within the affine subspace spanned by these points and that is equidistant from each of them. By this definition, we must have, for some $\alpha \in \mathbb{R}^m$,

$$\operatorname{circ}(x_0, x_1, x_2, \dots, x_m) = x_0 + \sum_{j=1}^m \alpha_j (x_j - x_0),$$

and, for all i ,

$$\|\operatorname{circ}(x_0, x_1, x_2, \dots, x_m) - x_i\| = \|\operatorname{circ}(x_0, x_1, x_2, \dots, x_m) - x_0\|.$$

These conditions lead to an $m \times m$ linear system in the vector of coefficients $\alpha \in \mathbb{R}^m$, where the i -th equation is

$$\sum_{j=1}^m \alpha_j \langle x_j - x_0, x_i - x_0 \rangle = \frac{1}{2} \|x_i - x_0\|^2,$$

or

$$\begin{pmatrix} \langle x_1 - x_0, x_1 - x_0 \rangle & \langle x_2 - x_0, x_1 - x_0 \rangle & \cdots & \langle x_m - x_0, x_1 - x_0 \rangle \\ \langle x_1 - x_0, x_2 - x_0 \rangle & \langle x_2 - x_0, x_2 - x_0 \rangle & \cdots & \langle x_m - x_0, x_2 - x_0 \rangle \\ \vdots & \vdots & \ddots & \vdots \\ \langle x_1 - x_0, x_m - x_0 \rangle & \langle x_2 - x_0, x_m - x_0 \rangle & \cdots & \langle x_m - x_0, x_m - x_0 \rangle \end{pmatrix} \begin{pmatrix} \alpha_1 \\ \alpha_2 \\ \vdots \\ \alpha_m \end{pmatrix} = \frac{1}{2} \begin{pmatrix} \|x_1 - x_0\|^2 \\ \|x_2 - x_0\|^2 \\ \vdots \\ \|x_m - x_0\|^2 \end{pmatrix}.$$

Solving this system determines the circumcenter $\text{circ}(x_0, x_1, x_2, \dots, x_m)$.

CRM in product space. Take $x_0 \in \mathbb{R}^n$ and define $z_0 = (x_0, x_0, \dots, x_0) \in \mathbb{R}^{nm}$. Let $W = U_1 \times U_2 \times \dots \times U_m$ and $D = \{(x, x, \dots, x) \in \mathbb{R}^{nm} : x \in \mathbb{R}^n\}$. For $z = (x^{(1)}, x^{(2)}, \dots, x^{(m)}) \in \mathbb{R}^{nm}$, the projection $P_D(z)$ of z onto D is given by

$$P_D(z) = \frac{1}{m} \left(\sum_{i=1}^m x^{(i)}, \sum_{i=1}^m x^{(i)}, \dots, \sum_{i=1}^m x^{(i)} \right)$$

while the projection $P_W(z)$ of z onto W is given by

$$P_W(z) = \left(P_{U_1}(x^{(1)}), P_{U_2}(x^{(2)}), \dots, P_{U_m}(x^{(m)}) \right).$$

The iterations of CRM in the product space $W \times D$ are given by

$$z^{k+1} = \text{circ}(z^k, R_W(z^k), R_D(R_W(z^k)))$$

where $R_W = 2P_W - I$ and $R_D = 2P_D - I$.

We say that a point y is an ε -approximate solution of the problem if $(y - y_i)^T Q_i (y - y_i) \leq (\eta_i + \varepsilon)^2$ for all i . All methods are run until an ε -approximate solution is found or until 10 minutes have elapsed without finding one. We call constraint violation at termination the quantity

$$\max_{i=1, \dots, m} (y - y_i)^T Q_i (y - y_i) - (\eta_i + \varepsilon)^2,$$

which should be nonpositive at termination, unless the method was run for at least 10 minutes without finding an ε -approximate solution.

The methods were implemented in Julia 1.11.5. Subproblems for projections were solved using Gurobi: 11.0.1 library. The code was run on an AMD Ryzen 5 2600 six-core processor with 24 GB of RAM. This code is available on github at <https://github.com/vguigues/3PM>.

We first run the methods for $m = 3$ ellipsoids in \mathbb{R}^2 . For this setup, we present in Figure 3 these three ellipsoids and represent the evolution of the iterates for all methods. As expected, all methods stop after finding a point in the intersection of the ellipsoids or very close to this intersection. The plot also represents the unit ball for the $\|\cdot\|_2$ -norm which, as we recall, is contained in all ellipsoids.

We now run the methods on 10 instances of our convex feasibility problem for $(m, n) = (3, 10)$, $(m, n) = (3, 50)$, $(m, n) = (3, 100)$, $(m, n) = (3, 1000)$, $(m, n) = (10, 100)$, $(m, n) = (10, 500)$, $(m, n) = (10, 1000)$, $(m, n) = (50, 500)$, $(m, n) = (50, 1000)$, $(m, n) = (100, 1000)$. For this experiment, we report in Tables 1 and 2, for the nine methods described before, namely 3PM, 3PM \parallel , A3PM, A3PM \parallel , Cyclic projections, Cimmino, Cimmino \parallel , SCCRM, and CRM, the number of iterations, the CPU time in seconds, and the constraint violation at termination. In these tables, we highlight in bold and in red the quickest method for all problem instance. We computed in these experiments an ε -approximate solution with $\varepsilon = 10^{-8}$. Some comments are now in order:

- A3PM or A3PM \parallel are the best methods in terms of CPU time, in 8 of the 10 instances.
- SCCRM is fastest in two instances, narrowly outperforming A3PM in one.
- Parallel implementations are in general quicker than their non-parallelized counterpart, but not always, due to the time required to distribute the computations in different threads.
- Cimmino and CRM are the worst methods in terms of CPU time in these instances.
- Though we have shown superlinear convergence of 3PM under some assumptions, in our instances 3PM did not perform well for large instances.

We also report in Figure 4 the evolution of the constraint violations along iterations for all methods and 5 of the instances. We observe that Cimmino and A3PM tend to use more iterations and the constraint violation decreases slower with these methods. SCCRM needs in general few iterations, though it can sometimes

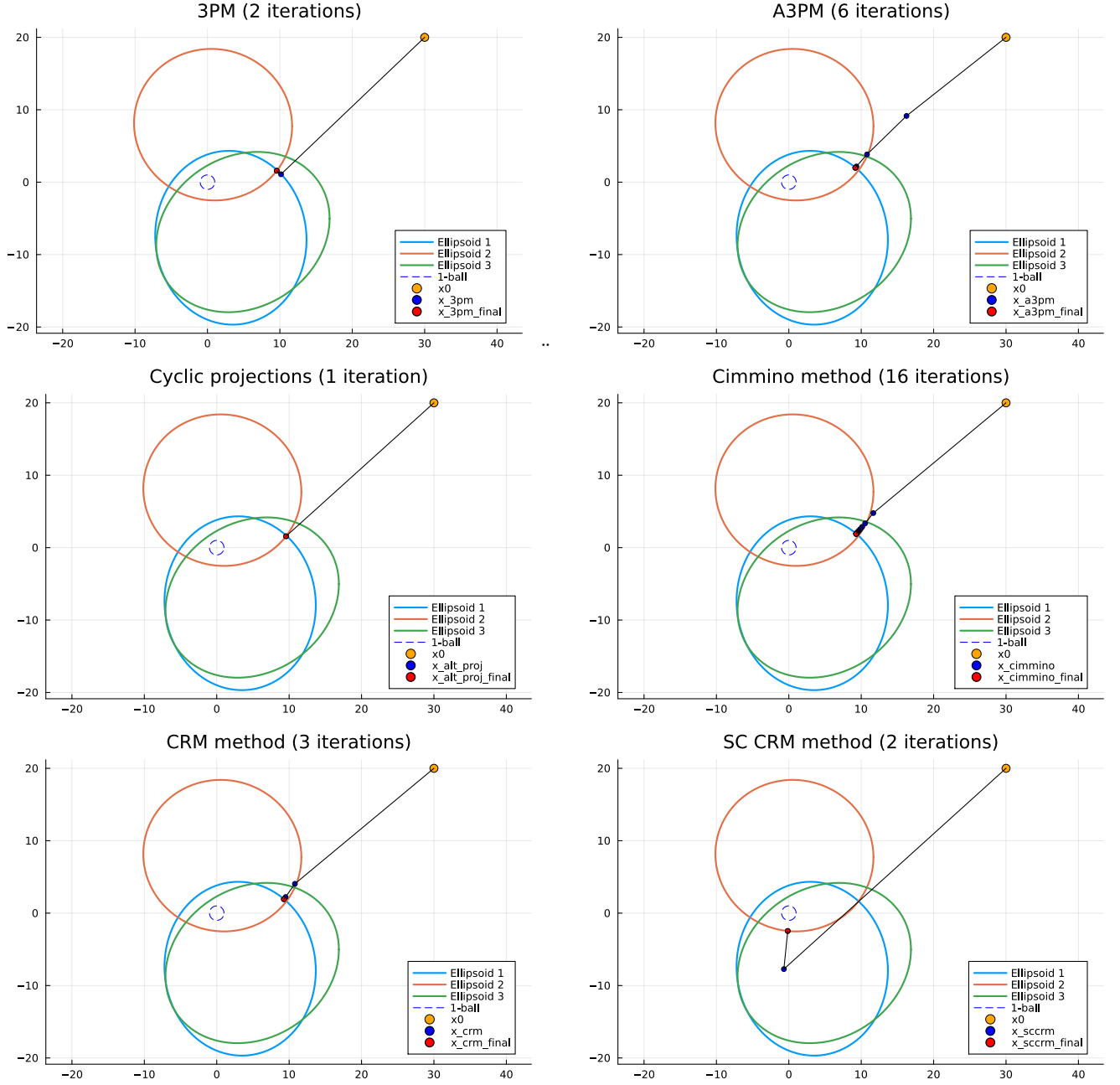


Figure 3: Illustration of 3PM, A3PM, cyclic projections, Cimmino's method, CRM, and SCCRM methods to find a point in the intersection of 3 ellipses in \mathbb{R}^2 .

Method	m	n	Iterations	CPU time (s)	Constraint violation
3PM	3	10	1	0.00337	-0.0025
3PM	3	10	1	0.00259	-0.0025
A3PM	3	10	7	0.00032	-0.7877
A3PM	3	10	7	0.00070	-0.7877
Cyclic	3	10	1	0.00218	-0.0025
Cimmino	3	10	48	0.05752	-7.5734
Cimmino	3	10	48	0.05009	-7.5734
SCCRM	3	10	2	0.01476	-0.0217
CRM	3	10	2	0.00688	-0.1923
3PM	3	50	3	0.05318	-56.3220
3PM	3	50	3	0.03118	-56.3220
A3PM	3	50	8	0.00098	-167.1852
A3PM 	3	50	8	0.00078	-167.1852
Cyclic	3	50	1	0.01374	-0.2105
Cimmino	3	50	1	0.01284	-415999.5440
Cimmino	3	50	1	0.00707	-415999.5440
SCCRM	3	50	1	0.02615	-89742.6906
CRM	3	50	4	0.08202	-1536.7657
3PM	3	100	3	0.14799	-2466.1367
3PM	3	100	3	0.08301	-2466.1366
A3PM	3	100	8	0.00806	-3386.0654
A3PM 	3	100	8	0.00170	-3386.0654
Cyclic	3	100	1	0.04907	-2.2873
Cimmino	3	100	18	0.42693	-228.6494
Cimmino	3	100	18	0.47930	-228.6494
SCCRM	3	100	2	0.10322	-41251.7301
CRM	3	100	3	0.25536	-19558.2516
3PM	3	1000	3	12.4355	-1.41e7
3PM	3	1000	3	9.2820	-1.41e7
A3PM	3	1000	5	0.1971	-1.18e7
A3PM	3	1000	5	0.3847	-1.18e7
Cyclic	3	1000	1	5.3111	-1.15e6
Cimmino	3	1000	1	5.4527	-1.21e9
Cimmino	3	1000	1	3.9068	-1.21e9
SCCRM	3	1000	1	7.0298	-3.59e8
CRM	3	1000	2	17.7935	-1.57e7
3PM	10	100	5	0.4371	-10088.9
3PM	10	100	5	0.3246	-10088.9
A3PM	10	100	9	0.0106	-4062.4
A3PM	10	100	9	0.2111	-4062.4
Cyclic	10	100	1	0.0683	-251.9
Cimmino	10	100	39	1.2540	-6397.1
Cimmino	10	100	39	1.2472	-6397.1
SCCRM	10	100	8	0.0884	-1870.3
CRM	10	100	4	0.6351	-1981.7

Table 1: Comparison on several instances (for several values of m and n) of the number of iterations, CPU time, and constraint violation at termination for 3PM, parallel 3PM (3PM ||), A3PM, parallel A3PM (A3PM ||), cyclic projections, Cimmino’s method, parallel Cimmino’s method (Cimmino ||), Successive Centralized CRM (SCCRM), and CRM using $\varepsilon = 10^{-8}$.

Method	m	n	Iterations	CPU time (s)	Constraint violation
3PM	10	500	3	6.7066	-1.3e6
3PM	10	500	3	5.0711	-1.3e6
A3PM	10	500	8	0.3801	-1.1e6
A3PM	10	500	8	0.4590	-1.1e6
Cyclic	10	500	1	1.9664	-20651.6
Cimmino	10	500	11	11.8282	-258241.8
Cimmino	10	500	11	8.2947	-258241.8
SCCRM	10	500	1	1.1339	-1.94e7
CRM	10	500	4	14.5173	-1.51e6
3PM	10	1000	2	35.7312	-3.1e7
3PM	10	1000	2	31.5069	-3.1e7
A3PM	10	1000	8	1.5014	-6.8e6
A3PM	10	1000	8	1.6410	-6.8e6
Cyclic	10	1000	1	12.2368	-2.2e7
Cimmino	10	1000	34	179.3706	-2.8e6
Cimmino	10	1000	34	161.6030	-2.8e6
SCCRM	10	1000	1	6.5463	-2.1e8
CRM	10	1000	3	67.8992	-6.9e7
3PM	50	500	3	37.6726	-3.7e6
3PM	50	500	3	30.4509	-3.7e6
A3PM	50	500	9	3.3924	-431986.7
A3PM 	50	500	9	2.3589	-431986.7
Cyclic	50	500	1	4.1694	-121892.8
Cimmino	50	500	1	19.7370	-7.8e7
Cimmino	50	500	1	17.5321	-7.8e7
SCCRM	50	500	49	9.6754	-73627.1
CRM	50	500	5	102.5789	-612568.5
3PM	50	1000	2	156.5059	-3.8e7
3PM	50	1000	2	147.1472	-3.8e7
A3PM	50	1000	8	8.2272	-4.2e6
A3PM	50	1000	8	7.4691	-4.2e6
Cyclic	50	1000	1	17.6827	-2.0e7
Cimmino	50	1000	15	605.2691	5.5e7
Cimmino	50	1000	29	600.4700	2.9e7
SCCRM	50	1000	1	7.3082	-2.1e8
CRM	50	1000	3	412.9610	-8.7e6
3PM	100	1000	2	358.8288	-3.6e7
3PM	100	1000	2	294.6009	-3.6e7
A3PM	100	1000	8	21.6928	-593678.9
A3PM	100	1000	8	17.3567	-593678.9
Cyclic	100	1000	1	24.4503	-4.4e7
Cimmino	100	1000	100	3118.5956	3.4e7
Cimmino	100	1000	100	2670.5723	3.4e7
SCCRM	100	1000	1	7.1063	-5.4e7
CRM	100	1000	3	873.6313	-9.4e6

Table 2: Comparison on several instances (for several values of m and n) of the number of iterations, CPU time, and constraint violation at termination for 3PM, parallel 3PM (3PM ||), A3PM, parallel A3PM (A3PM ||), cyclic projections, Cimmino’s method, parallel Cimmino’s method (Cimmino ||), Successive Centralized CRM (SCCRM), and CRM using $\varepsilon = 10^{-8}$.

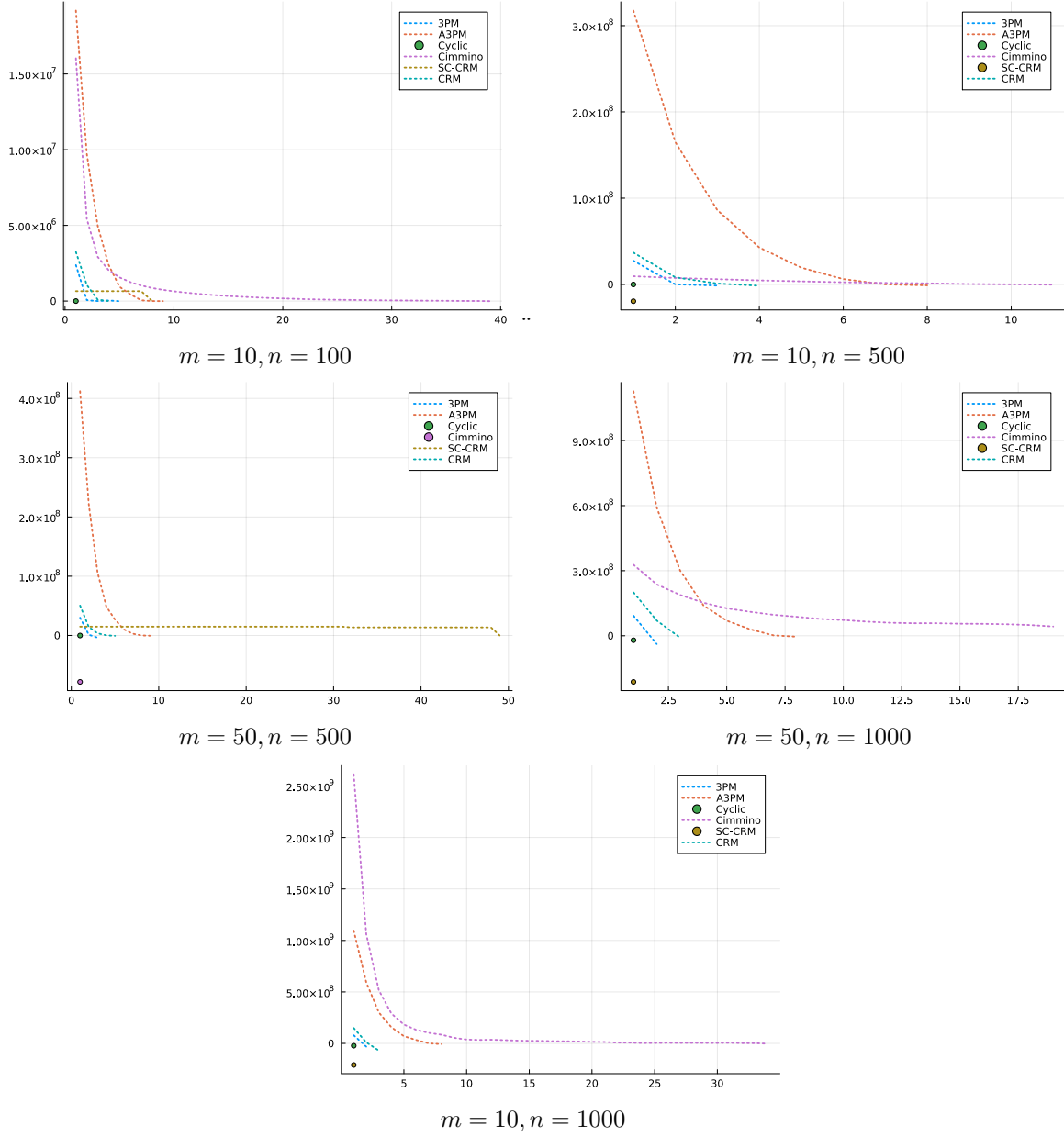


Figure 4: Evolution of the constraint violations along iterations of the methods for several instances of the convex feasibility problem with several values of the number m of sets and problem dimension n .

Problem sizes	3PM	3PM	A3PM	A3PM	Cyclic	Cimmino	Cimmino	SCCRM	CRM
$m = 3, n = 1000$	11.66	8.74	0.14	0.13	5.08	5.25	3.49	6.67	17.02
$m = 10, n = 100$	0.42	0.16	0.0068	0.0051	0.065	1.22	1.23	0.09	0.62
$m = 10, n = 500$	6.16	4.58	0.33	0.20	1.76	10.60	7.39	1.19	14.47
$m = 10, n = 1000$	34.87	28.80	1.15	0.93	12.08	177.74	150.59	6.64	67.69
$m = 50, n = 500$	28.27	22.68	2.04	1.75	3.20	14.83	11.99	6.90	88.14
$m = 50, n = 1000$	149.78	132.04	6.78	6.65	16.24	603.64	601.01	7.13	364.77
$m = 100, n = 1000$	270.92	242.79	13.27	11.23	19.94	706.82	646.04	7.12	757.34

Table 3: Comparison for several values of m and n of the average CPU time of all methods over 10 instances for $\varepsilon = 10^{-8}$.

Method	m	n	$\varepsilon = 100\,000$	$\varepsilon = 10\,000$	$\varepsilon = 10^{-3}$	$\varepsilon = 10^{-8}$
SCCRM	100	1000	6.8563	7.0134	7.2412	7.1063
A3PM	100	1000	5.3124	9.8971	12.9859	21.6928
A3PM	100	1000	3.4657	7.5412	11.1016	17.3567

Table 4: Comparison for $m = 100$ and $n = 1000$ of the CPU time for A3PM, A3PM ||, and SCCRM for several values of ε .

require a significant number of iterations before finding an ε -approximate solution, see the instance with $m = 50, n = 100$.

We then consider among the 10 instances chosen before the 7 largest and run each of the 9 methods ten times on these instances. For each instance and each method, we report in Table 3 the average CPU time (over the 10 runs) required to find an ε -approximate solution for $\varepsilon = 10^{-8}$. We report in red (resp. blue) and in bold the best (resp. second best) method in terms of CPU time. We see that A3PM and A3PM || are always either the best or second best in terms of CPU time with A3PM being the best in 6 of the 7 chosen problem instances. For $m = 50$ and $n = 1000$, in the corresponding experiment from Table 2, SCCRM was the fastest while it is now (when averaging the CPU time over 10 runs, as opposed to using a single run) the third best. For the largest instance, SCCRM is still the best, needing 7.12 seconds for convergence while the second best A3PM || needs 11.23 seconds. However, this experiment was still done with the high accuracy $\varepsilon = 10^{-8}$. Since every iteration of A3PM and A3PM || is very fast, we expect the CPU time with these methods to decrease significantly when ε increases and very few iterations are required. Therefore, we conducted the final following experiment: for the largest instance where SCCRM was the fastest with $\varepsilon = 10^{-8}$, we consider three other values of ε : $\varepsilon = 10^5$, $\varepsilon = 10^4$, and $\varepsilon = 10^{-3}$. The CPU time with A3PM, A3PM ||, and SCCRM for this largest instance and these values of ε is reported in Table 4, with the quickest CPU time reported in bold red for each value of ε . We observe that for the largest value of ε , both A3PM and A3PM || are now quicker than SCCRM. Therefore, A3PM or A3PM || were the quickest for all instances but one for solutions of high accuracy and the quickest on all instances if the accuracy is loose.

5 Concluding Remarks

We have proposed and analyzed the Parallel Polyhedral Projection Method (3PM) and its inexact variant A3PM for solving convex feasibility problems. The method combines the computational advantages of parallel projections with a geometric correction step via projection onto a polyhedron, leading to a simple yet powerful two-phase algorithm.

Theoretical results include global convergence under no regularity assumptions, linear convergence under a standard error bound condition, and superlinear convergence when the sets and iterations of the algorithm exhibit additional geometric regularity. These results remain valid even when projections are computed approximately, making the method robust in practical scenarios.

Numerical experiments demonstrate that A3PM outperforms several classical projection schemes, especially in multi-set settings, and scales favorably as the number of constraint sets increases.

References

- [1] F. J. Aragón Artacho, J. M. Borwein, and M. K. Tam. Recent results on douglas–rachford methods for combinatorial optimization problems. *Journal of Optimization Theory and Applications*, 163(1):1–30, 2014.
- [2] Francisco J. Aragón Artacho and Rubén Campoy. A new projection method for finding the closest point in the intersection of convex sets. *Computational Optimization and Applications*, 69(1):99–132, 2018.
- [3] Francisco J. Aragón Artacho, Yair Censor, and Aviv Gibali and. The cyclic douglas–rachford algorithm with r-sets-douglas–rachford operators. *Optimization Methods and Software*, 34(4):875–889, 2019.
- [4] Pablo Barros, Roger Behling, Vincent Guigues, and Luiz-Rafael Santos. Parallelizing the circumcentered reflection method, 2025. Preprint, available at <https://arxiv.org/abs/2505.17258>.
- [5] H. Bauschke and J. M. Borwein. On the convergence of von neumann’s alternating projection algorithm for two sets. *Set-Valued Analysis*, 1(2):185–212, 1993.
- [6] H. Bauschke and J. M. Borwein. On projection algorithms for solving convex feasibility problems. *SIAM Review*, 38(3):367–426, 1996.
- [7] H. Bauschke and Patrick L. Combettes. *Convex Analysis and Monotone Operator Theory in Hilbert Spaces*. Springer, Cham, 2nd edition, 2017.
- [8] H. Bauschke, Hao Ouyang, and Xianfu Wang. On circumcenters of finite sets in hilbert spaces. *Linear and Nonlinear Analysis*, 4:271–295, 2018.
- [9] H. Bauschke, Hao Ouyang, and Xianfu Wang. Best approximation mappings in hilbert spaces. *Mathematical Programming*, 195:855–901, 2022.
- [10] H. H. Bauschke, J. Y. Bello Cruz, T. T. A. Nghia, H. M. Phan, and X. Wang. Optimal rates of linear convergence of relaxed alternating projections and generalized douglas–rachford methods for two subspaces. *Numerical Algorithms*, 73(1):33–76, 2016.
- [11] H. H. Bauschke and W. M. Moursi. On the douglas–rachford algorithm. *Mathematical Programming*, 164(1-2):263–284, 2017.
- [12] R. Behling, J. Y. Bello-Cruz, and L. R. Santos. On the linear convergence of the circumcentered-reflection method. *Operations Research Letters*, 46(2):159–162, 2018.
- [13] R. Behling, J. Y. Bello-Cruz, and L. R. Santos. The block-wise circumcentered–reflection method. *Computational Optimization and Applications*, 76:675–699, 2020.
- [14] R. Behling, Y. Bello-Cruz, A. N. Iusem, and L. R. Santos. On the centralization of the circumcentered reflection method. *Mathematical Programming*, 205:337–371, 2024.
- [15] R. Behling, Y. Bello-Cruz, and L. R. Santos. Circumcentering the douglas–rachford method. *Numerical Algorithms*, 78(3):759–776, 2018.
- [16] R. Behling and Y. Bello-Cruz and L.R. Santos. On the circumcentered-reflection method for the convex feasibility problem. *Numerical Algorithms*, 86:1475–1494, 2021.
- [17] Jonathan M. Borwein and Brailey Sims. The douglas–rachford algorithm in the absence of convexity. In *Fixed-Point Algorithms for Inverse Problems in Science and Engineering*, pages 93–109. Springer, New York, 2011.

- [18] G. Cimmino. Calcolo approssimato per le soluzioni dei sistemi di equazioni lineari. *Ricerca Scientifica*, 9(II):326–333, 1938.
- [19] P. L. Combettes. The convex feasibility problem in image recovery. In P. W. Hawkes, editor, *Advances in Imaging and Electron Physics*, volume 95, pages 155–270. Elsevier, San Diego, 1996.
- [20] P.L. Combettes and J.-C. Pesquet. Proximal splitting methods in signal processing. In H.H. Bauschke, R.S. Burachik, P.L. Combettes, V. Elser, D.R. Luke, and H. Wolkowicz, editors, *Fixed-Point Algorithms for Inverse Problems in Science and Engineering*, volume 49 of *Springer Optimization and Its Applications*, pages 185–212. Springer, 2011.
- [21] Iain S. Duff, Ronan Guivarch, Daniel Ruiz, and Mohamed Zenadi. The augmented block cimmino distributed method. *SIAM Journal on Scientific Computing*, 37(3):A1248–A1269, 2015.
- [22] M. Fukushima. An outer approximation algorithm for solving general convex programs. *Operations Research*, 31(1):101–113, 1983. Accessed: 25 Apr. 2025.
- [23] Deren Han, Yansheng Su, and Jiabin Xie. Randomized douglas–rachford methods for linear systems: Improved accuracy and efficiency. *SIAM Journal on Optimization*, 34(1):1045–1070, 2024.
- [24] Victor I. Kolobov, Simeon Reich, and Rafał Zalas. Finitely convergent deterministic and stochastic iterative methods for solving convex feasibility problems. *Mathematical Programming*, 194(1):1163–1183, 2022.
- [25] Alexander Y. Kruger. About intrinsic transversality of pairs of sets. *Set-Valued and Variational Analysis*, 26(1):111–142, 2018.
- [26] G. Li and T. K. Pong. Douglas–rachford splitting for nonconvex optimization with application to nonconvex feasibility problems. *Mathematical Programming*, 159:371–401, 2016.
- [27] Tianle Lu and Xue Zhang. An inertial parametric douglas–rachford splitting method for nonconvex problems. *Mathematics*, 12(5), 2024.
- [28] Ion Necoara, Peter Richtárik, and Andrei Patrascu. Randomized projection methods for convex feasibility: Conditioning and convergence rates. *SIAM Journal on Optimization*, 29(4):2814–2852, 2019.
- [29] H. M. Phan. Linear convergence of the douglas–rachford method for two closed sets. *Optimization*, 65(2):369–385, 2016.
- [30] A. Iusem D. Liu R. Behling, Y. Bello-Cruz and L-R Santos. A successive centralized circumcentered-reflection method for the convex feasibility problem. *Computational Optimization and Applications*, 87:83–116, 2024.
- [31] R. Tyrrell Rockafellar. *Convex Analysis*. Princeton Landmarks in Mathematics and Physics. Princeton University Press, Princeton, NJ, 10th edition, 1997.
- [32] H. D. Scolnik, N. Echebest, M. T. Guardarucci, et al. Incomplete oblique projections for solving large inconsistent linear systems. *Mathematical Programming*, 111:273–300, 2008.
- [33] J. Shen, J. S. Chen, H. D. Qi, et al. A penalized method of alternating projections for weighted low-rank hankel matrix optimization. *Mathematical Programming Computation*, 14:417–450, 2022.
- [34] F. Sukru Torun, Murat Manguoglu, and Cevdet Aykanat. Enhancing block cimmino for sparse linear systems with dense columns via schur complement. *SIAM Journal on Scientific Computing*, 45(2):C49–C72, 2023.
- [35] J. Wang, Y. Hu, C. Li, and J.-C. Yao. Linear convergence of cq algorithms and applications in gene regulatory network inference. *Inverse Problems*, 33(5):055017, 2017.